



Publication Year	2020
Acceptance in OA @INAF	2023-10-06T09:52:00Z
Title	Optical thermal filters for eXTP: Manufacturing and characterization
Authors	Chen, Tianxiang; Gao, Na; Chen, Yong; Xu, Yupeng; Lu, Fangjun; et al.
DOI	10.1117/12.2562041
Handle	http://hdl.handle.net/20.500.12386/34441
Series	PROCEEDINGS OF SPIE
Number	11444

PROCEEDINGS OF SPIE

[SPIDigitalLibrary.org/conference-proceedings-of-spie](https://spiedigitallibrary.org/conference-proceedings-of-spie)

Optical thermal filters for eXTP: manufacturing and characterization

Chen, Tianxiang, Gao, Na, Chen, Yong, Xu, Yupeng, Lu, Fangjun, et al.

Tianxiang Chen, Na Gao, Yong Chen, Yupeng Xu, Fangjun Lu, Jiewei Cao, Xiongwei Xu, Ugo Lo Cicero, Marco Barbera, Marco Feroci, "Optical thermal filters for eXTP: manufacturing and characterization," Proc. SPIE 11444, Space Telescopes and Instrumentation 2020: Ultraviolet to Gamma Ray, 114448E (13 December 2020); doi: 10.1117/12.2562041

SPIE.

Event: SPIE Astronomical Telescopes + Instrumentation, 2020, Online Only

Optical thermal filters for eXTP: Manufacturing and characterization

Tianxiang Chen^a, Na Gao^a, Yong Chen^a, Yupeng Xu^a, Fangjun Lu^a, Jiewei Cao^a, Xiongwei Xu^b,
Ugo Lo Cicero^c, Marco Barbera^d, Marco Feroci^e

^aInstitute of High Energy Physics, China; ^bChangchun University of Science and Technology, China;
^cINAF - Osservatorio Astronomico di Palermo "Giuseppe Salvatore Vaiana", Italy; ^dUniv. Degli
Studi di Palermo, Italy; ^eINAF - Istituto di Astrofisica e Planetologia Spaziali, Italy

ABSTRACT

In order to ensure the effective detection of X-ray astronomical detectors by blocking ultraviolet, visible and infrared light, adding optical thermal filter in front of the load is an effective method. According to the scientific requirements of eXTP, optical thermal filters with aluminized polyimide (PI) film structure had been designed and tested in this paper, the results of mechanical tests including burst pressure, vibration and acoustic tests, also the transparent properties of optics in UV, Vis and IR lights are presented. The mechanical test results show that the filters for LAD and SFA can't pass the acoustic tests, causing the thickness of PI should be increased or a nickel mesh structure should be added. Furthermore, the transmission test results indicate that a single-sided Al deposited structure is more suitable than a double-sided one.

Keywords: Optical thermal filter, Vibration test, Acoustic test, Burst pressure, Transparent property.

1. INTRODUCTION

The core scientific goal of the enhanced X-ray Timing and Polarimetry (eXTP) mission is to research the new physical processes and laws in black holes and neutron stars, including general relativity under extreme gravitational conditions, quantum chromodynamics under extreme density conditions, and quantum electrodynamics under extreme magnetic field conditions, which can be summarized as: "one odd (black hole), two stars (neutron star and quark star), three extremes (extreme gravitation, extreme magnetic field and extreme density)".^[1]

The enhanced X-ray Timing and Polarimetry (eXTP) mission is a space mission with 4 scientific payloads: the spectroscopy focusing array (SFA), the large area detector (LAD), the polarimetry focusing array (PFA) and the wide field monitor (WFM).^[2]

Optical thermal filters are critical items in the mission. They are used in SFA, PFA and LAD payloads to block the UV, Vis and IR lights to protect the optics and maintain the thermal stability of the system.

The optical thermal filters are composed by PI and Al layers and supported by nickel frames. The filters not only need to be strong enough to resist the vibration and acoustic environment during the launch, but also thin enough to allow a maximum X-ray transmission. The filter size is large (near 120 mm × 80 mm in different shapes), and in particular the filters for SFA and PFA which are placed in front of the mirror module are very thin (<600 nm, include PI and Al). To design a filter that can resist the violent launch mechanical environment is a great challenge.

The design of filter used in LAD is shown in Figure 1. The thickness of the PI film is 2 μm±200 nm, while the thickness of the Al film is 200 nm±20 nm; the overall filter size is 112.4×73.9 mm, while the effective filter size is 108.8×70.2 mm.

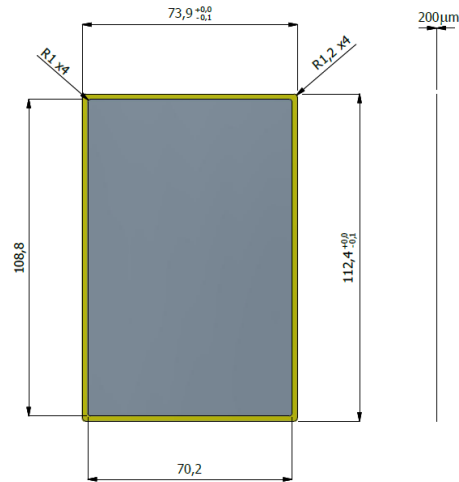


Figure 1. Filter design drawing for LAD

Because the sizes of X-ray grazing-incidence Wolter-I (parabola + hyperbola) optics modules are same for SFA and PFA, the sizes of filters mounted before the optics modules are same for these two payloads. We just discuss the filters for SFA, The filters in front of the SFA optics modules were made up of multiple small fan-shaped filters. The installation diagram is shown in Figure 2. In order to ensure the transmittance of low-energy soft X-rays, the PI thickness of the filters for SFA is designed to be 400nm, and the thickness of the Al film is designed to be 80nm. Figure 3 shows that the actual size of one small filter.

The actual filter prototypes for LAD and SFA payload are showed in Figure 4.

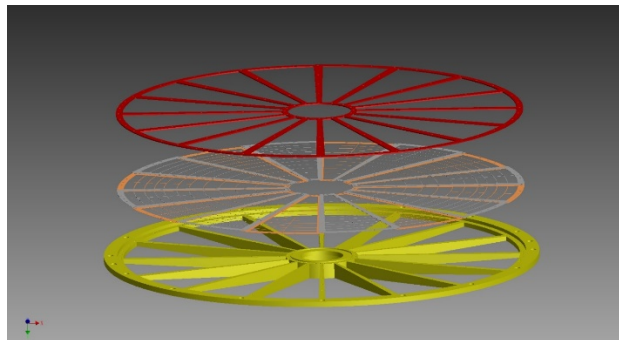


Figure 2 . Installation of filters in front of SFA optics modules.

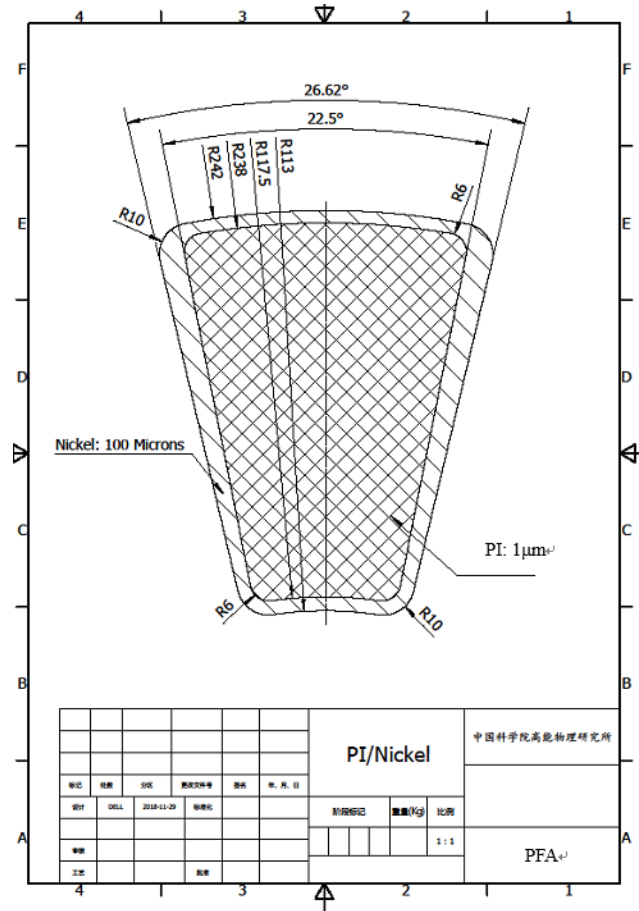


Figure 3. Filter design drawing for SFA

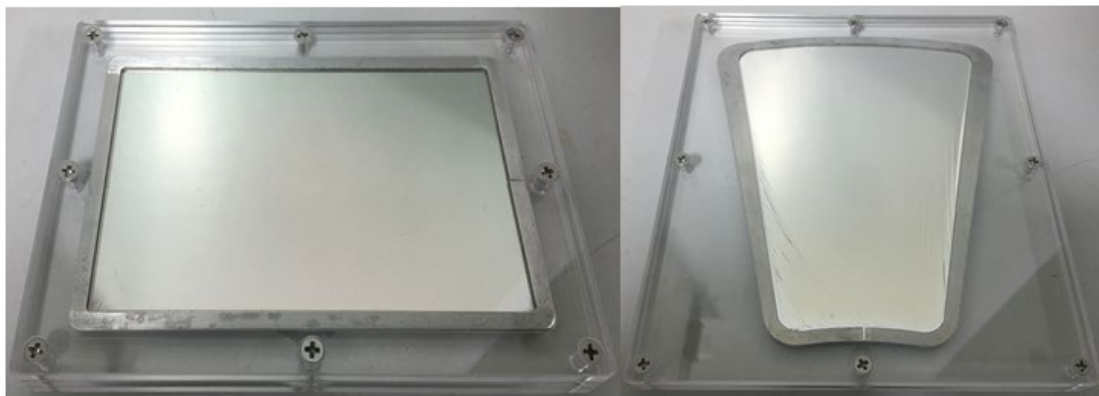


Figure 4. Actual filter prototypes for LAD (left) and SFA (right).

In this presentation, we present our results of mechanical tests including burst pressure, vibration and acoustic tests, also the transparent properties of filters in UV, Vis and IR lights. A study of optimizing the filter manufacturing process is also underway to ensure the filter survival during the mission launch.

2. PREPARATION PROCESS OF FILTERS

2.1 Materials and Structure

The optical thermal filter is composed with PI layer, Al layer and supporting nickel frame in structure. The schematic diagram of the structure is shown in Figure 5. The main function of the Al film is to block UV, Vis and IR lights, and the main function of the PI film is to support and strengthen the Al film. In addition, the PI film has a strong absorption of UV light. The main function of the nickel frame is to support the entire filter and to match and install with other equipment.



Figure 5. Schematic diagram of thermal filters.

2.2 Preparation of PI Film

The PI film is made by spin coating method. One can coat polyamic acid solution on a silicon wafer, and convert the polyamic acid film into a PI film by thermal imidization method. The polyamic acid solution is synthesized by dissolving dihydric (BPDA) and diamine (PDA) in the polar solvent DMAc under ice bath conditions. The reaction process is shown in Figure 6. The efficacious method to control the thickness and uniformity of the PI film is to change the viscosity of the solution, the spin coating time and rotation speed.

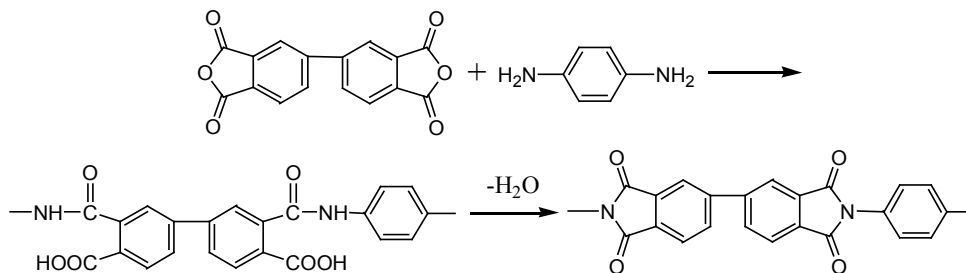


Figure 6. Schematic diagram of PI prepared by BPDA and PDA.

2.3 Preparation of Nickel Frame

The nickel frame is prepared by the method of micro electroplating. The thickness of nickel frame can be controlled by changing the electroplating time and current.

2.4 Preparation of Al Film

The Al film is vapor-deposited by magnetron sputtering on the surface of the PI film supported with nickel mesh.

3. MECHANICAL TESTS OF THE FILTERS

The optical thermal filter should be strong enough to resist the vibration and acoustic environment during the launch. In order to characterize the mechanical properties of the thermal filters, vibration and acoustic tests had been carried out. A simple method of measuring the burst pressure of thermal filters to characterize the mechanical properties of the filters has been proposed.

3.1 Vibration and Acoustic Tests

Two filters for LAD and two filters for SFA had been prepared for vibration and acoustic tests. The information of these samples and six other small circular filters to measure the optical properties of the filters before and after the tests, is shown in Table 1. One filter for EP-FXT and two filters for HERMES were also involved in the mechanical tests. In this paper we won't discuss them.

Table 1. The design parameters of the LAD, SFA and 6 circular filters

Filter	Thickness of PI	Thickness of Al
LAD	800nm	120nm
SFA	400nm	120nm
1#	160nm	80nm
2#	160nm	80nm
3#	450nm	40nm
4#	1 μ m	80nm
5#	1 μ m	80nm
6#	400nm	80nm

All filters are fixed in the test fixture, as shown in Figure 7(left). Then vibration and acoustic tests are carried out. The conditions of vibration test are shown in Table 2 and 3.

Table 2. Sinusoidal vibration conditions

Direction	Frequency range (Hz)	Acceleration/amplitude 0~P	
		Appraisal level	Acceptance level
X、Y、Z	5-15	13.5mm	9.0mm
	15-85	12g	8g
	85-100	10g	6.7g
Scan rate		Each direction: 2 Oct/min	Each direction: 4 Oct/min

Table 3. Random vibration conditions

Frequency range (Hz)	Power Spectral Density (g ² /Hz)	
	Appraisal level	Acceptance level
10~100	+3dB/oct	+3dB/oct
100~600	0.125	0.05
600~2000	-9dB/oct	-9dB/oct
Root mean square acceleration	10.14g	6.41g
Time	2min	1min
Direction	X、Y、Z	X、Y、Z

The results of vibration tests are satisfactory. After completing the Z-direction appraisal-level sinusoidal and random vibration tests, visually observe that all filters are not damaged. In the same way, after completing the X, Y-direction appraisal-level sinusoidal and random vibration tests, visually observe that all the filters are not damaged. It means that all the 10 samples passed the appraisal-level tests, as shown in Figure 7(middle). 2# and 5# circular samples were taken off from the fixture to measure the transparent properties.

The acoustic test was carried out after the vibration test. The condition of the acoustic test is shown in Table 4. Appraisal-level condition is loaded in the test.

Table 4. Acoustic test condition

Frequency range (Hz)	Sound pressure level (dB) reference sound pressure amplitude: 2×10^{-5} Pa		
	Acceptance level	Appraisal level	Tolerance (dB)
31.5	120	124	-2 ~ +4
63	126	130	-2 ~ +4
125	131	135	-2 ~ +4
250	137	141	-2 ~ +4
500	135	139	-2 ~ +4
1000	133	137	-2 ~ +4
2000	126	130	-2 ~ +4
4000	122	127	-5 ~ +5
8000	115	119	-5 ~ +5
Total sound pressure level	141	145	-1 ~ +2
Time	1 min	2 min	
Sound field	Reverberation field		

The filters for SFA are too thin with such a large size, causing them all damaged. In order to improve the mechanical properties, some mesh should be added to support the SFA filter. The filters for LAD are much thicker than the filters for SFA. One filter is intact, while the other is damaged. So in the latest design the thickness of the filters for LAD has been changed to 2 um to ensure the filters survive in the acoustic environment. 1#, 3#, 4#, 6# circular samples are intact, as shown in Figure 7 (right).

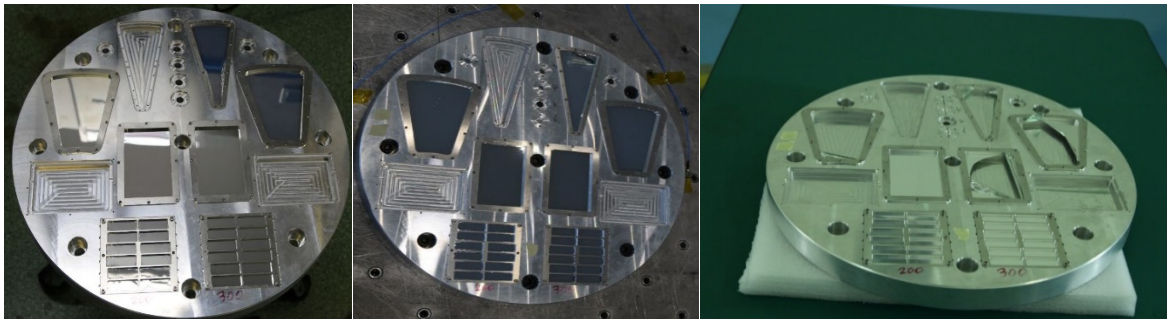


Figure 7. Picture of the samples during the vibration and acoustic test. (The left one is the samples before test, the middle one is the samples after vibration test, the right one is the samples after acoustic test)

In the same way, we tested the transparent properties of the left 4 circular samples. The results of the entire 6 circular filters are shown in Figure 8. As we can see, there is no difference between the two spectral line in each figure.

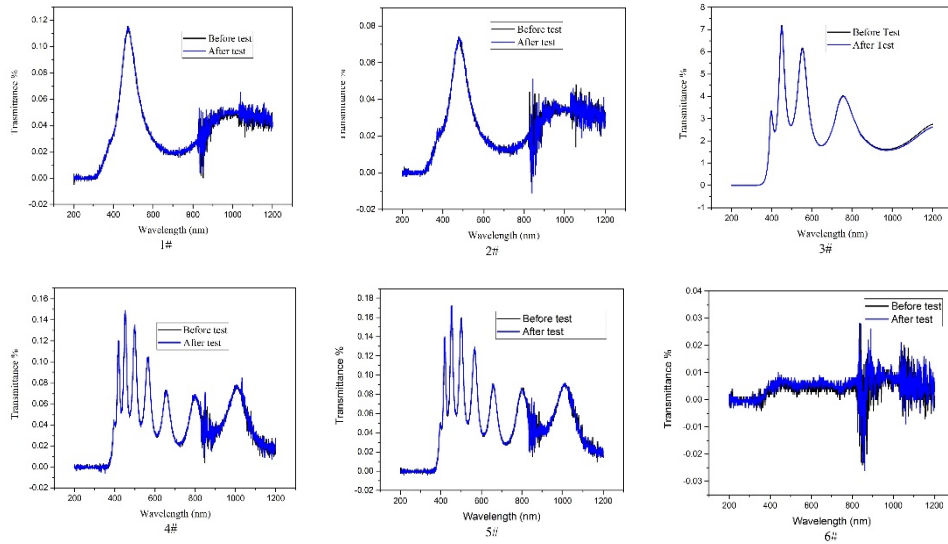


Figure 8. Changes in the optical properties of the filters before and after the mechanical test (1#, 3#, 4#, 6# are undergone vibration and acoustic test, 2# and 5# are undergone only vibration test)

3.2 Burst pressure Tests

The test above-mentioned is the most convincing test for the satellite engineering, but it will consume too much manpower and material resources, which is not suitable for the development stage testing and rapid testing. Burst pressure measurement can quickly help us test and verify the qualification of samples, which is suitable for film testing in the development stage.

The burst pressure test device is made up with one gas tank and one gas outlet which has two installation position. The sample installation position and the high-precision pressure gauge are symmetrically distributed on both sides of the gas outlet of the pressure tank to ensure equal pressure on both sides. By filling nitrogen into the tank to increase the pressure, forming a pressure difference with the atmospheric pressure, one can test the mechanical properties of the film, and the value of the pressure can be read in the high-precision pressure gauge.

Our samples are prepared and tested in batches. The preparation process is still in accordance with the aforementioned process in this article, but the specific parameters may be changed to prepare samples, which will be used as a comparative test to optimize the design.

The first batch of samples are prepared to test the mechanical properties with different thicknesses of PI. All these samples have no nickel mesh support, and the effective test size are all $\varnothing 16$ mm. As shown in Figure 9. The measured thickness and the data of the burst pressure that can withstand are displayed in Table 5.

Table 5. The burst pressure of the first batch of samples.

PI thickness (nm)	3474	2912	2462	2159	1740	1484	1261	1101
Burst pressure (Bar)	1.38	0.92	1.09	0.84	0.65	0.67	0.64	0.57

There is no doubt that the thinner the PI film is, the smaller the burst pressure. This batch of data can be used as a good comparison of subsequent data of samples with nickel mesh.

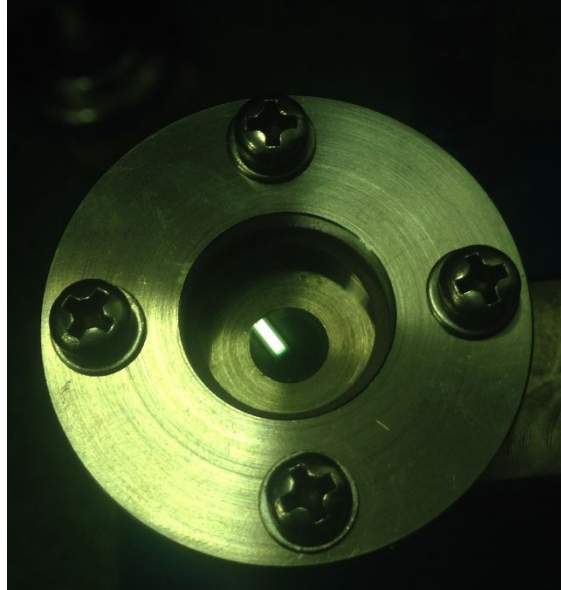


Figure 9. Thermal filter with no Ni mesh

The second batch of samples is to fix the thickness of the PI film (400 nm) and change the thickness of the supporting nickel mesh to verify the influence of the thickness of the nickel mesh on the burst pressure. The mesh is hexagonal, with a side length of 1mm. Nickel mesh with different thickness was prepared by electroplating. The measured Ni mesh thickness, mesh side width and the data of the burst pressure are displayed in Table 6.

Table 6. The burst pressure of the second batch of samples.

Ni mesh thickness(um)	8.0	14.6	23.3	34.0	39.2	41.3
Ni mesh side width(um)	100	110	120	130	150	155
Burst pressure (Bar)	0.0736	0.0952	0.8869	1.1354	1.1293	1.2284

For the samples with thinner nickel mesh (8.0 and 14.6 μm), a small pressure value will cause greater stress and finally break the thinner part of the nickel mesh, which will cause damage to the filter film. When the thickness of the nickel mesh further increases to 23.3 μm and 34.0 μm , the unevenness of the nickel mesh will be reduced, and the thinner defects in the nickel mesh decrease. However, the strength of the nickel mesh is still the main factor for the damage of the filter. As shown in Figure 10 (left), we can see that the nickel mesh is regionally damaged, which means the nickel mesh is not firm. When the thickness of the nickel mesh is increased to more than 39.2 μm , the unevenness of the nickel mesh is further reduced. The strength of the nickel mesh becomes a secondary factor contribute to the rupture. Instead, the strength of PI film itself becomes the main factor. At this time, the characteristic phenomenon of filter film damage is the damage of the PI film in a certain hexagonal small mesh, as shown in Figure 10 (right).

Therefore, for a 400nm PI film with 1mm-side-length hexagonal nickel mesh, when the thickness of the nickel mesh thinner than 40 μm , the nickel mesh isn't strong enough to support. The nickel mesh will rupture before the PI film, which is the main affecting of the burst pressure. When the thickness of the nickel mesh is thicker than 40 μm , the strength of the PI film becomes the main factor affecting the burst pressure test. But if there are still defects in the nickel mesh itself, the nickel mesh may still rupture before the PI membrane, which becomes the main factor affecting the burst pressure test. The burst pressure vs nickel thickness is shown in Figure 11.

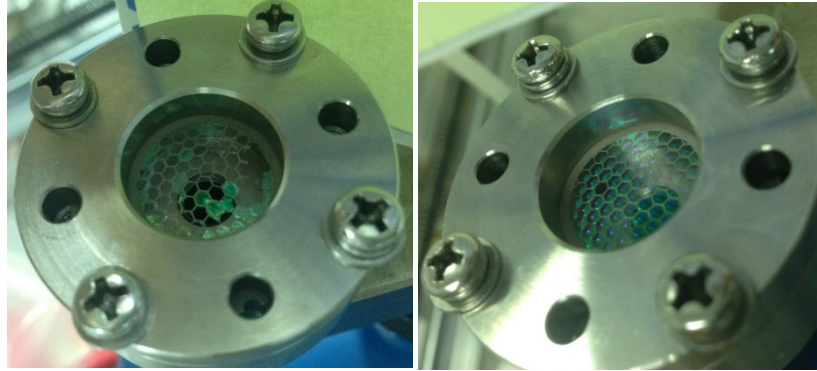


Figure 10. Regional rupture phenomenon (left) and Hexagonal hole damage (right)

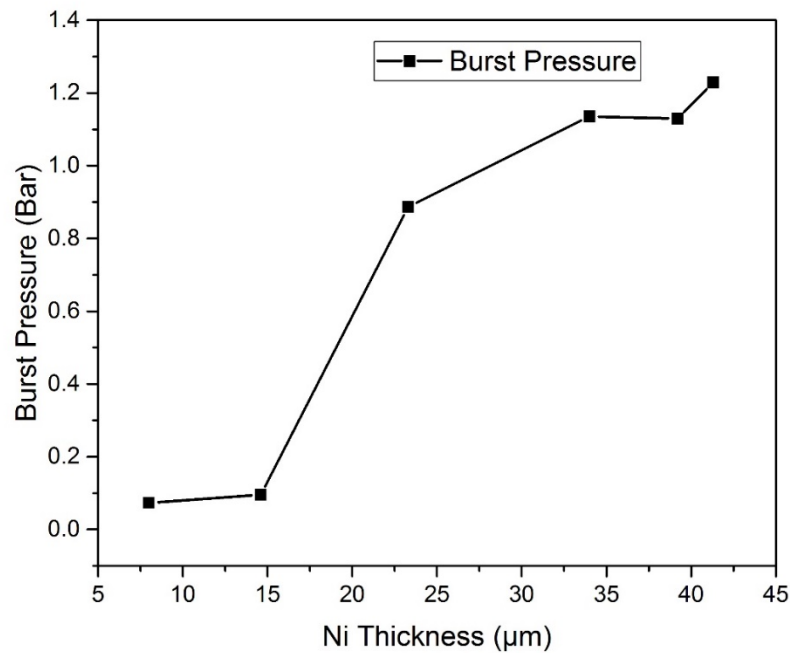


Figure 11. The burst pressure vs nickel mesh thickness.

The third batch of samples is to fix the thickness of the nickel mesh which is greater than 60μm, and change the thickness of PI films. The measured thickness of PI films and the burst pressure are displayed in Table 7. The burst pressure vs PI thickness is shown in Figure 12.

Table 7. The burst pressure of the third batch of samples.

PI thickness(nm)	587	520	400	328	211	157
Burst pressure (Bar)	1.7496	1.9611	1.7940	1.0672	0.6835	0.1397

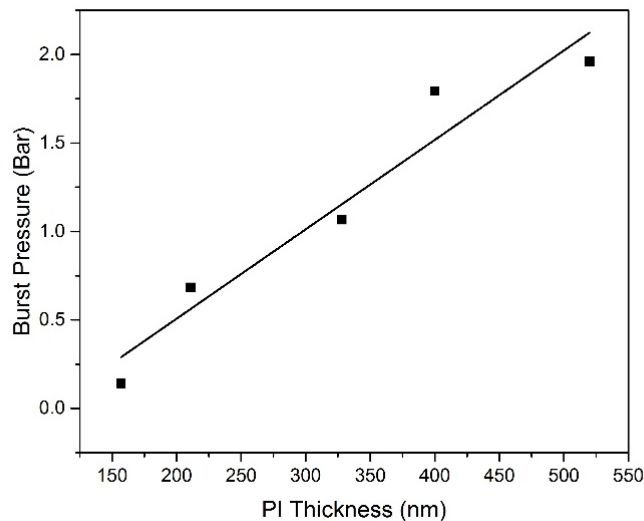


Figure 12. The burst pressure vs PI thickness

According to Table 7 and Figure 12, we can get the following conclusions. By using 1mm-side-length hexagonal nickel mesh support, the PI film thickness just needs to be greater than 328nm that can resist a differential pressure greater than 1 atmosphere. The 328nm-thickness of PI film has a high transmittance in the soft X-ray band, and this type of filter can be used for low-energy soft X-ray filtering. It can be seen from the test results of 5 samples that the burst pressure is basically linear with the thickness. The quality of the nickel mesh is still a key factor affecting the results of burst pressure.

4. OPTICAL TEST OF THE FILTERS

4.1 Method

In order to fully understand the transmittance of the aluminized PI filter, we tested the transmittance of different thickness of filters, which are single-sided or double-sided aluminized in the PI film.

An UV spectrophotometer (UV3600-PLUS) had been used to test our filters. The tested wavelength range is 200nm-1200nm, covering UV, Vis and IR bands. The thicknesses of PI film is 1 μ m with two different preparation process of Al film: single-sided and double-sided. For the case of single-sided Al deposited, 1 μ m PI film with different thicknesses of Al films (50nm, 60nm, 80nm, 100nm and 120nm) has been tested the transmittance. For the case of double-sided Al deposited, we compared the transmittance among the 80nm and 120nm Al films on single or double surfaces of PI with different thicknesses. The results of the optical tests are respectively shown in Figure 13, 14 and 15.

4.2 Results

A brief result is shown here, more detail results was shown in a previous paper.^[3] As shown in Figure 13, we can see the transmittance changes with different thicknesses of Al films on single-side of 1 μ m PI surface. When the thickness of the Al film is 50nm, the transmittance is less than 0.6%. As the thickness of the Al film increases, the transmittance gradually decreases. When the thickness of the Al film reaches 120nm, the transmittance value is already lower than the detection limit of the spectrophotometer, the detection signal is completely annihilated by the noise signal. The blocking effect of the filter increased with the thickness of Al layer, which proved that the Al layer can block the visible light effectively.

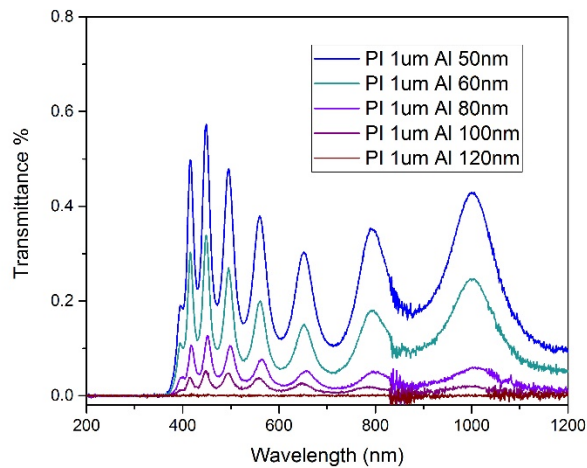


Figure 13. Transmittance results of filters with different Al thickness on one side of 1um PI surface.

As shown in Figure 14, we studied the influence of single-sided or double-sided Al (80nm) deposited on the surface of 1um PI on transmittance. For the double-sided Al deposited on the PI surface, since the two interfaces of the PI are both Al films, the interference light will increase at certain wavelengths, resulting in high transmittance. But when the PI surface is coated with Al on one side, there will be much lower interference light between Al film and air, and there will not be half wave loss effect. So, on the one hand, the peak value of transmittance of double-sided evaporation is entirely higher than the single-sided, and on the other hand, the peak and valley values of the transmittance curves of single-sided Al deposited and double-sided Al deposited are exactly opposite. For the filters with 120nm Al film on the single-sided and double-sided surface of 1um PI. It can be seen that the transmittance of the single-sided filter has been lower than the minimum detection limit of the spectrophotometer, but when Al on double sides, many clear transmittance peaks can still be observed at certain wavelengths.

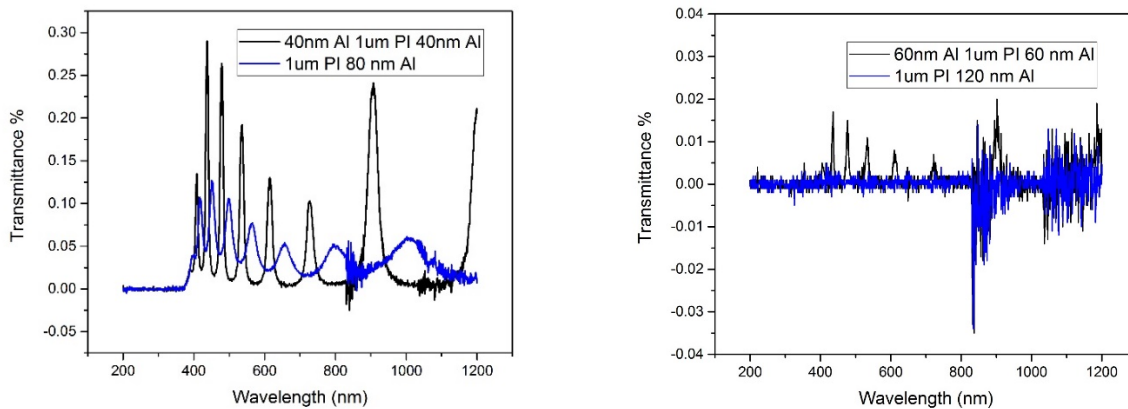


Figure 14. The different transmittance of filters with 80 nm (left) and 120 nm (right) Al deposited on single-sided or double-sided of PI surface

5. CONCLUSION

So far, all the mechanical and optical tests are finished. The final conclusions are as follows:

- (1) All thermal filters can pass the appraisal-level vibration test. However, the filters for SFA fail the appraisal-level acoustic test, and the filters for LAD partly fail the appraisal-level acoustic test. Knowing that increasing the thickness of PI or adding a nickel mesh can both increase the mechanical performance of the filter, the further design is in progress. Both vibration test and acoustic test have no effect on the optical performance of the filter.
- (2) With the increase of the thickness of single PI film, the maximum of burst pressure is increase. However, single PI film is too thick for the transmission of X-ray. After adding the mesh structure to the filter, the thickness of PI can be decreased to the hundreds of nanometers. A suitable size of filter with nickel mesh structure for requirement had been explored out.
- (3) The blocking effect increased with the thickness of Al layer. So the filter should have Al film as thick as possible. Otherwise, the filter should have a transmittance in the visible light band as uniform as possible, and the overall transmittance should be kept at a very low level, so single-sided Al deposition should be selected rather than double-sided.

REFERENCE

- [1] in 't Zand, J. J. M., Bozzo, E., Qu, J. L., et al., "Observatory science with eXTP", *Sci. China-Phys. Mech. Astron.*, 62, 029506 (2019).
- [2] Zhang, S. N., Santangelo, A., Feroci, M., et al., "The enhanced X-ray Timing and Polarimetry mission-eXTP", *Sci. China-Phys. Mech. Astron.*, 62, 029502 (2019).
- [3] Chen, T.X., Gao, N., Li, L., Chen, Y., Xu, Y.P., Lu, F.J., "Optical property characterization of optical blocking filters used in space X-ray survey", *Opti. Precision Eng.*, 27(11), 2337-2342 (2019).